J. Fluid Mech. (1983), *vol.* 136, *pp.* 453–466
Printed in Great Britain

A parabolic equation for the combined refraction–diffraction of Stokes waves by mildly varying topography

By JAMES T. KIRBY† AND ROBERT A. DALRYMPLE
Department of Civil Engineering, University of Delaware, Newark, DE 19711

(Received 8 February 1983 and in revised form 24 May 1983)

A parabolic equation governing the leading-order amplitude for a forward-scattered Stokes wave is derived using a multiple-scale perturbation method, and the connection between the linearized version and a previously derived approximation of the linear mild slope equation is investigated. Two examples are studied numerically for the situation where linear refraction theory leads to caustics, and the nonlinear model is shown to predict the development of wave-jump conditions and significant reductions in amplitude in the vicinity of caustics.

1. Introduction

For many applications to coastal and offshore problems, consideration of the surface wave field can be restricted to an initially plane wave moving in a given direction. In this case, parabolic-equation approximations can be constructed which consider only the unidirectional wave and the forward-scattered components arising from interaction with structures or inhomogeneities of the domain. The parabolic equation may be derived by employing a WKB-type expansion for the velocity potential representing a wave travelling in a prespecified direction; substitution into the equations of motion and the assumption of slowly varying or constant depth then leads to an equation governing modulations of the wave amplitude. Such an approach has been made (for linearized wave theory) by Liu & Mei (1976), who studied waves shoaling on a plane beach and interacting with shore-attached or shore-parallel breakwaters, and by Mei & Tuck (1980), who studied waves diffracted by slender obstacles in water of otherwise constant depth.

Alternatively, Radder (1979) demonstrated a method for obtaining coupled parabolic equations for forward- and back-scattered waves by employing a splitting-matrix approach to the linear mild-slope elliptic model of Berkhoff (1972), given by

$$\nabla_h \cdot (CC_g \nabla_h \tilde{\phi}) + \omega^2 \frac{C_g}{C} \tilde{\phi} = 0, \tag{1.1}$$

where ∇_h is a gradient operator in horizontal coordinates (x, y), ω is the angular frequency, $\tilde{\phi}(x, y)$ is a two-dimensional velocity potential obtained by factoring out the harmonic time dependence, and C and C_g are the phase and group velocities respectively. Recently, Liu & Tsay (1983*a*) have described a method for obtaining the back-scattered wave by an iterative procedure, using coupled equations similar

† Present address: Marine Sciences Research Center, State University of New York, Stony Brook, New York 11794.

to those obtained by Radder. Comparison of numerical applications of the linear parabolic method to laboratory data can be found in Lozano & Liu (1980), Berkhoff, Booij & Radder (1982) and Tsay & Liu (1982).

Using the WKB expansion approach in the context of Stokes theory, Yue & Mei (1980) obtained a parabolic equation for the propagation of weakly nonlinear Stokes waves in a specified direction in water of constant depth. The resulting nonlinear Schrödinger equation is given by

$$2\mathrm{i}A_x+\frac{1}{k}A_{yy}-K'|A|^2A=0,$$

where x is the principal direction of propagation and A is a complex amplitude. In the present study we arrive at a more general formulation governing waves in a domain with slow but arbitrary depth variations. This nonlinear mild-slope equation is obtained in § 2 by extending the multiple-scale perturbation expansion of Yue and Mei to the case of non-constant depth. Then, in §3, we demonstrate the connection between the resulting nonlinear parabolic equation and a linear model obtained by using Radder's (1979) parabolic approximation of (1.1). In §4 we present a numerical approximation using the Crank–Nicolson algorithm, and study two cases illustrating nonlinear amplitude modulations induced by topographic refraction.

2. The parabolic approximation for refraction–diffraction

We consider the combined refraction and diffraction of an initially plane Stokes wave with frequency ω, reference wavenumber k_0, and amplitude A_0, approaching from $-\infty$ at a small angle to the x-axis. The exact equations for the velocity potential ϕ and the free surface η, assuming inviscid irrotational flow, are given by

$$\nabla^2\phi=0 \quad (-h<z<\eta(x,y,t)), \tag{2.1a}$$

$$g\phi_z+\phi_{tt}+|\nabla\phi|_t^2+\tfrac{1}{2}(\nabla\phi\cdot\nabla)|\nabla\phi|^2=0 \quad (z=\eta(x,y,t)), \tag{2.1b}$$

$$\phi_t+g\eta+\tfrac{1}{2}|\nabla\phi|^2=0 \quad (z=\eta(x,y,t)), \tag{2.1c}$$

$$\phi_z=-\nabla_{\mathrm{h}}\phi\cdot\nabla_{\mathrm{h}}h \quad (z=-h(x,y)). \tag{2.1d}$$

Here g is the gravitational acceleration and ∇ represents the three-dimensional gradient operator.

We proceed by performing a multiple-scale perturbation expansion and expanding the free-surface boundary conditions (2.1b, c) about $z=0$ in Taylor series. The derivation follows closely the work of Yue & Mei (1980).

2.1. *Lengthscales and perturbation expansions*

We seek a nonlinear equation governing the amplitude A of a modulated Stokes wave, whose potential may be written in the form

$$\phi=-\frac{\mathrm{i}g}{2\omega}A(x,y)f(x,y,z)\,\mathrm{e}^{\mathrm{i}(k_0x-\omega t)}+\text{c.c.}+O(\epsilon^2), \tag{2.2}$$

where A is $O(\epsilon)$, ϵ represents the Stokes-wave steepness parameter, and c.c. denotes the complex conjugate. k_0 is a reference wavenumber given by the initial conditions of the wave field. The water depth h is allowed to be a slowly varying function of the horizontal coordinates x and y; consequently A must be allowed to be a complex

function in order to absorb the difference between the reference phase $k_0 x - \omega t$ and the actual phase $\psi(k(x,y))$. We choose two scales for x given by

$$\frac{\partial}{\partial x} \sim \frac{\partial}{\partial x} + \epsilon^2 \frac{\partial}{\partial X}, \tag{2.3}$$

where x relates to the wavelike characteristics and $X = \epsilon^2 x$ covers the slower spatial variations of the remaining term Af. It is assumed that no fast wave-like variations occur in the y-direction, consistent with the forward scattering approach; A is allowed to vary at $O(\epsilon)$ in the y-direction to account for slow modulations due to small but finite angles of propagation with respect to the x-axis:

$$\frac{\partial}{\partial y} \sim \epsilon \frac{\partial}{\partial Y}. \tag{2.4}$$

These scales form the basis of Yue & Mei's approach. The problem is further considered to be steady; only fast derivatives in t, related to the frequency, are considered.

A scale for $\nabla_h h$ must be chosen in order to determine the point at which the term in $\nabla_h h$ enters the bottom boundary condition. In Chu & Mei (1970), $\nabla_h h$ is assumed to be $O(\epsilon)$, giving rise to primary solutions at $O(\epsilon^2)$ which affect wave phase and speed through terms related to the changes in depth, amplitude and wavenumber. Here, in keeping with a mild-slope approximation, we restrict $\nabla_h h$ to $O(\epsilon^2)$; the bottom is then effectively locally flat up to the third order in ϵ. Correspondingly, we allow

$$\frac{\partial k}{\partial x} \sim \epsilon^2 \frac{\partial k}{\partial X}, \quad \frac{\partial f}{\partial x} \sim \epsilon^2 \frac{\partial f}{\partial X}, \tag{2.5}$$

where f is given by

$$f(X, Y_1, z) = \frac{\cosh k(h+z)}{\cosh kh}. \tag{2.6}$$

In the y-direction we define an additional scale $Y_1 = \epsilon^2 y$, so that

$$\frac{\partial f}{\partial y} \sim \epsilon^2 \frac{\partial f}{\partial Y_1}. \tag{2.7}$$

This condition will be relaxed somewhat below.

Perturbation series of the form

$$\phi = \sum_{n=1} \epsilon^n \sum_{m=-n}^{n} \phi_{mn}(x,y,z)\, \mathrm{e}^{\mathrm{i}m\psi}, \tag{2.8a}$$

$$\eta = \sum_{n=1} \epsilon^n \sum_{m=-n}^{n} \eta_{mn}(x,y)\, \mathrm{e}^{\mathrm{i}m\psi}, \tag{2.8b}$$

where

$$\psi = \int^x k\, \mathrm{d}x - \omega t, \tag{2.9}$$

and k is a local wavenumber, are substituted into (2.1), giving a boundary-value problem in z for each order of m and n:

$$\left(\frac{\partial^2}{\partial z^2} - m^2 k^2\right) \phi_{mn} = F_{mn} \quad (-h < z < 0), \tag{2.10a}$$

$$\left(g\frac{\partial}{\partial z} - m^2\omega^2\right) \phi_{mn} = G_{mn} \quad (z = 0), \tag{2.10b}$$

$$-g\eta_{mn} = H_{mn} \quad (z = 0), \tag{2.10c}$$

$$\frac{\partial \phi_{mn}}{\partial z} = B_{mn} \quad (z = -h), \tag{2.10d}$$

where F_{mn}, G_{mn}, H_{mn}, B_{mn} are determined by lower-order solutions. For $n = 1$ and 2, $m = 1$, the problems are homogeneous. The solution for ϕ_{11} is given by

$$\phi_{11} = -\frac{ig}{2\omega} f A' e^{i\psi} + \text{c.c.}, \tag{2.11a}$$

where c.c. is the complex conjugate and A' is referenced to the local wavenumber, with

$$\omega^2 = gk \tanh kh. \tag{2.11b}$$

Here k is based on the local value of h. The homogeneous solution ϕ_{12} of identical form is neglected. At $m = 1$, $n = 3$, a homogeneous solution of the form (2.11a) arises for the inhomogeneous problem, leading to the solvability condition

$$\int_{-h}^{0} F_{13} f \, dz + \frac{B_{13}}{\cosh kh} = \frac{G_{13}}{g}, \tag{2.12}$$

as in Chu & Mei (1970). G_{13} is identical with the result in Yue & Mei, and can be written as

$$G_{13} = \frac{i\omega^3 k}{2 \tanh kh} D |A'|^2 A', \tag{2.13}$$

where

$$D = \frac{\cosh 4kh + 8 - 2\tanh^2 kh}{8 \sinh^4 kh}. \tag{2.14}$$

B_{13} is new here, and is given by

$$B_{13} = -\phi_{11x}|_{-h} \frac{\partial h}{\partial X} - \phi_{11y}|_{-h} \frac{\partial h}{\partial Y}, \tag{2.15}$$

while F_{13} is slightly modified from Yue & Mei (1980) to include the spatial derivatives of k and f:

$$F_{13} = -2\phi_{11xX} - ik_X \phi_{11} - \phi_{11YY}, \tag{2.16}$$

where it is understood that the slow X-derivative of ϕ_{11} does not operate on k. Note that, in deriving B_{13} and F_{13}, we allow f_Y to appear as a term at $O(\epsilon)$. This has the effect of including a smaller term in the formulation, which is acceptable. In addition, for a wave whose direction deviates significantly from x, the contribution of ϕ_{11Y} approaches $O(1)$; in this extreme, the $O(\epsilon^2)$ variation of f_{Y1} enters the scheme naturally. Finally, it will be shown that the inclusion of the $O(\epsilon^2)$ quantity is consistent with a previously derived model.

2.2. *The approximate equation*

The governing equation for the forward-scattering parabolic approximation is obtained by substituting (2.13), (2.15) and (2.16) into the solvability condition (2.12). The boundary terms in B_{13} are cancelled by terms arising from Leibnitz differentiation in the integral of F_{13}. Performing the integral over depth and noting that

$$\int_{-h}^{0} f^2 \, dz = \frac{CC_g}{g}, \tag{2.17}$$

where $C = \omega/k$ and $C_g = \partial\omega/\partial k$, leads to a nonlinear equation governing the complex amplitude A':

$$2ikCC_g A'_X + i(kCC_g)_X A' + (CC_g A'_Y)_Y - kCC_g K' |A'|^2 A' = 0, \tag{2.18}$$

where

$$K' = k^3 \left(\frac{C}{C_g}\right) D, \tag{2.19}$$

as given in Yue & Mei (1980). The amplitude is now phase-shifted by the substitution

$$A' = A\,\mathrm{e}^{\mathrm{i}(k_0 x - \int^x k\,\mathrm{d}x)}, \tag{2.20}$$

yielding solutions of the form

$$\phi = -\frac{\mathrm{i}g}{2\omega} A f\,\mathrm{e}^{\mathrm{i}(k_0 x - \omega t)} + \text{c.c.} + O(\epsilon^2). \tag{2.21}$$

Substituting (2.20) into (2.18) gives

$$2\mathrm{i}kCC_{\mathrm{g}} A_X + 2k(k-k_0)(CC_{\mathrm{g}})A + \mathrm{i}(kCC_{\mathrm{g}})_X A + (CC_{\mathrm{g}} A_Y)_Y - k(CC_{\mathrm{g}})K'|A|^2 A = 0, \tag{2.22}$$

which is the final form for the parabolic approximation.

3. Comparison with previously derived models and extensions

In this section we explore the correspondence of the nonlinear mild-slope equation (2.22) to the previously derived models of Radder (1979) and Yue & Mei (1980).

3.1. *Parabolic approximation of Radder* (1979), *for linear waves*

Employing a splitting-matrix method described by McDaniel (1975) and Corones (1975), Radder (1979) constructed a parabolic equation for $\tilde{\phi}$ given by

$$\tilde{\phi}_x - \mathrm{i}k\tilde{\phi} + \frac{1}{2kCC_{\mathrm{g}}}(kCC_{\mathrm{g}})_x \tilde{\phi} - \frac{\mathrm{i}}{2kCC_{\mathrm{g}}}(CC_{\mathrm{g}}\tilde{\phi}_y)_y = 0, \tag{3.1}$$

where $\tilde{\phi}(x, y)$ is the potential at $z = 0$ governed by (1.1), and where it is assumed that the waves are propagating at a small angle to the $+x$-direction. Here coupling between forward- and back-scattered wave components has been neglected. After substituting for $\tilde{\phi}$ by

$$\tilde{\phi} = -\frac{\mathrm{i}g}{\omega} A\,\mathrm{e}^{\mathrm{i}k_0 x}, \tag{3.2}$$

consistent with (2.21), (3.1) becomes

$$2\mathrm{i}kCC_{\mathrm{g}} A_x + 2k(k-k_0)CC_{\mathrm{g}} A + \mathrm{i}(kCC_{\mathrm{g}})_x A + (CC_{\mathrm{g}} A_y)_y = 0, \tag{3.3}$$

which is identical with the result obtained by linearizing (2.22). The nonlinear model is thus seen to correspond to the level of approximation obtained by using a splitting method on the more general (but linear) wave equation (1.1) which allows wave propagation in any direction. Conversely, it is seen that the approximations made in obtaining (3.1), embodied in Radder's (1979) choice of splitting matrix, are consistent with the multiple-scale ordering scheme presented in §2.

3.2. *Pure diffraction*

Simplification of the nonlinear equation (2.22) to the case of constant depth leads to the nonlinear Schrödinger equation given by Yue & Mei (1980):

$$2\mathrm{i}k_0 A_x + A_{yy} - k_0 K'|A|^2 A = 0. \tag{3.4}$$

Yue & Mei showed that this equation predicts the essential features of the development of the Mach stem in the case of nonlinear waves incident at glancing angles on a vertical wall. Peregrine (1983) has shown that (3.4) may be cast in a form analogous to the equation governing the development of an undular hydraulic jump. The presence of a Mach stem thus indicates a jump discontinuity between two

conjugate wave states, with the jump to the conjugate state replacing the normal process of simple reflection and superposition in a linear wave field.

4. Numerical examples of combined refraction–diffraction

In this section we study several examples where the refraction approximation to linear theory predicts the occurrence of caustics and cusps of caustics, along which the amplitude is singular. It is well known that equations of the form (1.1) provide uniformly valid solutions in these regions due to the incorporation of diffraction effects (see Meyer 1979). In cases where the caustics are oriented at a sufficiently small angle to the computational direction x to allow for forward-scattered reflection into the computational domain, parabolic approximations also provide a qualitatively accurate approximation of the behaviour near the singularity for waves of low steepness (see Radder 1979; Berkhoff *et al.* 1982). For the case of the nonlinear model, the combined refraction–diffraction process may lead to the formation of wave jumps as in the constant-depth case, in regions where refraction leads to the superposition of rays and formation of singularities in the linear refraction approximation.

4.1. *Numerical approximations*

Both the nonlinear equation (2.22) and its linearized counterpart are approximated according to the Crank–Nicolson scheme. Application of the scheme to the nonlinear model (2.22) yields the difference equation

$$\left\{1+\frac{(pk)_j^{i+1}-(pk)_j^i}{2\alpha_j}+\mathrm{i}\Delta x\left\{\frac{p_{j+1}^{i+1}+2p_j^{i+1}+p_{j-1}^{i+1}}{4(\Delta y)^2\alpha_j}+\frac{k_0-k_j^{i-1}}{2}+\frac{K_j'^{i+1}}{4}|\tilde{A}_j^{i+1}|^2\right\}\right\}A_j^{i+1}$$

$$-\frac{\mathrm{i}\Delta x}{4\Delta y^2\alpha_j}\{(p_{j+1}^{i+1}+p_j^{i+1})A_{j+1}^{i+1}+(p_j^{i+1}+p_{j-1}^{i+1})A_{j-1}^{i+1}\}$$

$$=\left\{1-\frac{((pk)_j^{i+1}-(pk)_j^i)}{2\alpha_j}-\mathrm{i}\Delta x\left\{\frac{(p_{j+1}^i+2p_j^i+p_{j-1}^i)}{4(\Delta y)^2\alpha_j}+\frac{k_0-k_j^i}{2}-\frac{K_j'^i}{4}|A_j^i|^2\right\}\right\}A_j^i$$

$$+\frac{\mathrm{i}\Delta x}{4(\Delta y)^2\alpha_j}\{(p_{j+1}^i+p_j^i)A_{j+1}^i+(p_j^i+p_{j-1}^i)A_{j-1}^i\}+O(\Delta x^2,\Delta y^2), \tag{4.1}$$

where

$$\alpha_j=(pk)_j^{i+1}+(pk)_j^i, \tag{4.2}$$

$$p_j^i=C_j^iC_{gj}^i, \tag{4.3}$$

$$x_i=(i-1)\Delta x, \tag{4.4a}$$

$$y_j=(j-1)\Delta y. \tag{4.4b}$$

The scheme (4.1) is used in an iterative manner, where, for the first iteration, $\tilde{A}_j^{i+1}$ is given by A_j^i. Then for the second iteration, $\tilde{A}_j^{i+1}$ is given by the intermediate value resulting from the first step.

For the linear model (3.3) the nonlinear terms are dropped from (4.1), and the Crank–Nicolson scheme proceeds without iteration.

Initial conditions for both models are given on $x=0$ by

$$A_j^i=A_0 \quad (i=1, \quad 1\leqslant j\leqslant N), \tag{4.5}$$

implying normal wave incidence on the upwave grid boundary. The initial wave amplitude is given by A_0, and N is the number of grid points in the y-direction. The

lateral boundaries at $y = 0$, $(N-1)\Delta y$ are taken to be reflective (either due to symmetry or for a boundary located far from the region of interest)

$$\frac{\partial A}{\partial y} = 0 \quad (y = 0, \quad (N-1)\Delta y), \tag{4.6}$$

which is approximated by

$$A_1^i = A_2^i, \quad A_{N-1}^i = A_N^i \quad (1 \leqslant i \leqslant M). \tag{4.7}$$

In the case of an open boundary it is understood that computation will be terminated at a value of $x_i = (M-1)\Delta x$ before diffracted waves are significantly reflected back into the region of interest.

4.2. *Submerged circular shoal*

As a first example we study the case of a submerged circular shoal on a bottom of otherwise constant depth, studied by Radder (1979). Configuration 1 of Radder's paper is used, with

$$\frac{h_{\mathrm{M}}}{R} = 0.0625, \quad \frac{h_0}{R} = 0.1875, \quad \frac{L_0}{R} = 0.5,$$

where R is the shoal radius and L_0 is the incident wavelength given by $L_0 = 2\pi/k_0$. The depth h is given by

$$h = h_{\mathrm{M}} + e_0 r^2 \quad (r < R), \tag{4.8a}$$

$$h = h_0 \quad (r \geqslant R), \tag{4.8b}$$

where

$$r^2 = (x-x_{\mathrm{M}})^2 + (y-y_{\mathrm{M}})^2, \tag{4.8c}$$

$$e_0 = (h_0 - h_{\mathrm{M}})/R^2. \tag{4.8d}$$

In this example the rays of a linear refraction approximation are focused into a cusped caustic. Peregrine (1983) has discussed the likely form of results for the weakly nonlinear approximation, and has shown that a situation analogous to the Mach stem studied above can occur, in which two jumps in wave conditions fan out in approximately the same manner as the caustics emanating from the region of the cusp. The region between the jump conditions, directly in the lee of the submerged shoal, would then be dominated by waves of approximately uniform amplitude propagating in the incident-wave direction.

For the shoal studied here, the constant-depth region $r \geqslant R$ is characterized by $k_0 h_0 = 2.36$. The variation of the normalized amplitude along the line of symmetry $y/R = 0$, where x is the incident wave direction, is shown in figure 1 for values of $k_0 A_0 = 0.16$ and 0.32, and for the linear theory. For both cases, a significant reduction of the maximum amplitude in the neighbourhood of the cusp is seen, with the reduction increasing with nonlinearity. In figure 2 the normalized amplitude in the y-direction is plotted for the initial value $k_0 A_0 = 0.32$ at locations $x/R = 2.9, 4.2, 5.5$ and 6.8. The results clearly show the growth of a central region bounded by jumps located on the $+y$ and $-y$ sides. These results are in qualitative similarity with the results of the Mach reflection studied by Yue & Mei, with the exception that the presence of intersecting wavetrains is induced by refraction of the incident wave rather than reflection. A weaker jump was also noted for the less-nonlinear case $k_0 A_0 = 0.16$, with the jumps spreading at a smaller angle to the x-axis and with larger wave amplitude in the central focused region. For smaller initial wave steepnesses, the results are qualitatively similar to the linear results presented in figure 2.

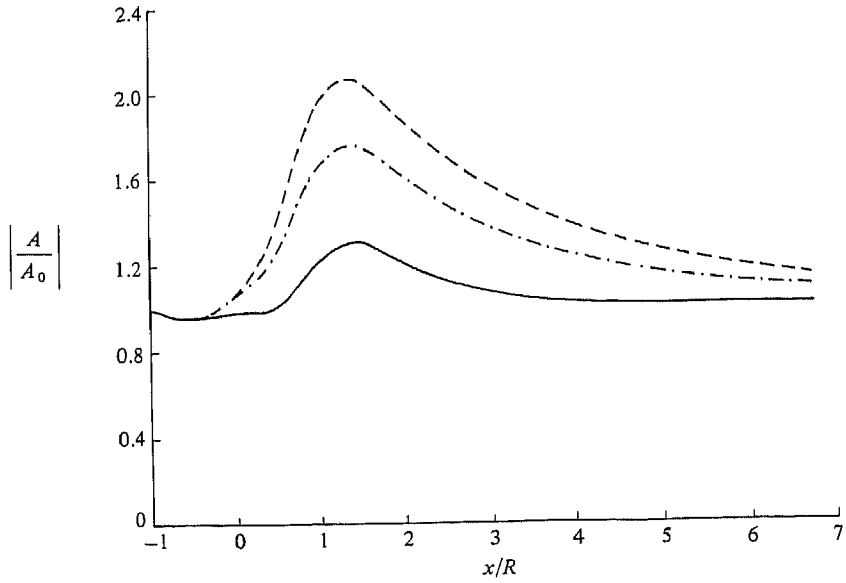

FIGURE 1. Circular shoal; amplitude along centreline: ——, linear result; –·–·–, $k_0 A_0 = 0.16$; ——, $k_0 A_0 = 0.32$.

Owing to the large angle formed between the wave jump and the x-axis for the case of $k_0 A_0 = 0.32$, insufficient wave energy is incident on the wedge between the jumps to maintain the amplitude of the jump. This result is qualitatively similar to the results presented by Yue (1980) for waves in the vicinity of a curved wedge of parabolic form which bends away from the initial jump, where the distance between the wall and nearly straight jump boundary increases too rapidly for the maintenance of uniform amplitude and a partial shadow is formed adjacent to the wall. Wave energy near the jump is thus gradually diffracted into this region, resulting in a region of low waves in comparison to the vicinity of the jump.

4.3. *Reflection from a linear caustic*

As a second example we study the incidence of a plane wave in constant water depth on a symmetric wedge-shaped depression, with sides sloping down from the constant-depth region. The line of symmetry is taken as $y = 0$. The boundary of the depression is given by

$$y_b = x \tan \alpha, \tag{4.9}$$

where α is the wedge angle, and where $x = 0$ represents the tip of the wedge, and the bottom slopes down with a slope of 1:50 normal to the boundary. The maximum depth of the depression is given by $2h_0$. The incident wave is characterized by $k_0 h_0 = 1.0$ in the constant-depth region outside the wedge. For the cases considered, a caustic of the linear wave field occurs on the sloping boundary, and, in the far field (x large) the wave field in the vicinity of the caustic would be described by an Airy function, with an exponentially decaying amplitude in the geometric shadow and total reflection of the incident wave. The corresponding result for weakly nonlinear waves would be a qualitatively similar description in terms of the second Painlevé transcendent (Miles 1978). However, Peregrine (1983) has suggested that the development of a wave field in the vicinity of the caustic may be greatly dependent

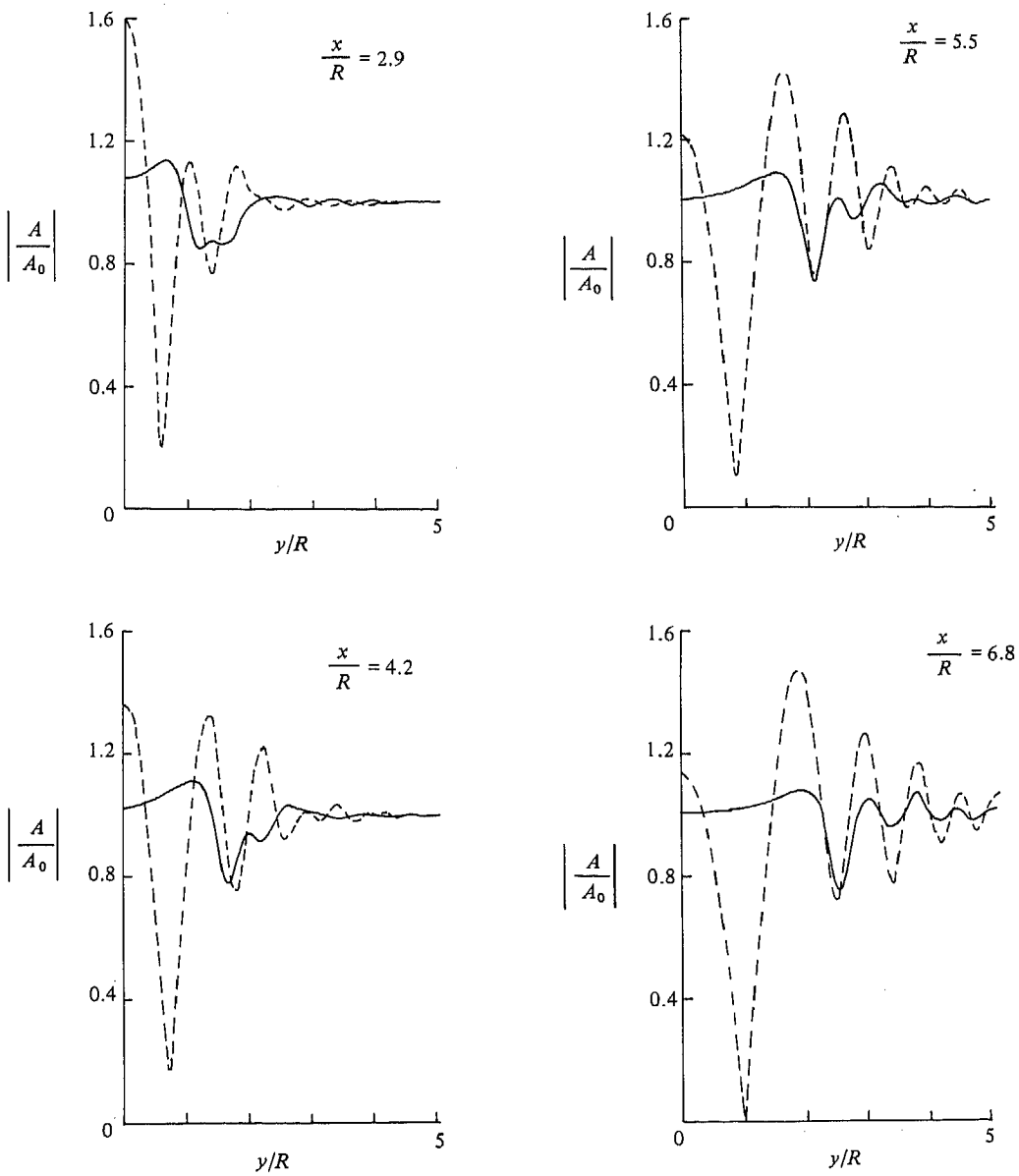

FIGURE 2. Normalized amplitude *vs.* distance from centreline; circular shoal: ---, linear result; ——, $k_0 A_0 = 0.32$, solution of (2.22).

on the initial conditions, and the asymptotic state in qualitative similarity to the Airy function of linear theory may not result, particularly in the event that a jump condition with little or no reflection of the incident wave occurs.

As a test of this hypothesis, two geometries given by $\alpha = 15°$ and $\alpha = 25°$ were tested, with incident wave steepnesses of $k_0 A_0 = 0.1$ and 0.2. Results for $\alpha = 15°$ and $\alpha = 25°$ are presented in comparison to linear theory in figures 3 and 4 respectively, where normalized amplitude perpendicular to the line of symmetry $y = 0$ are plotted for $k_0 x = 40$, 80, and 120. For the case of $\alpha = 15°$ and $k_0 A_0 = 0.1$ (figure 3*a*), the nonlinear wave field evolves in a qualitatively similar manner to the linear waves,

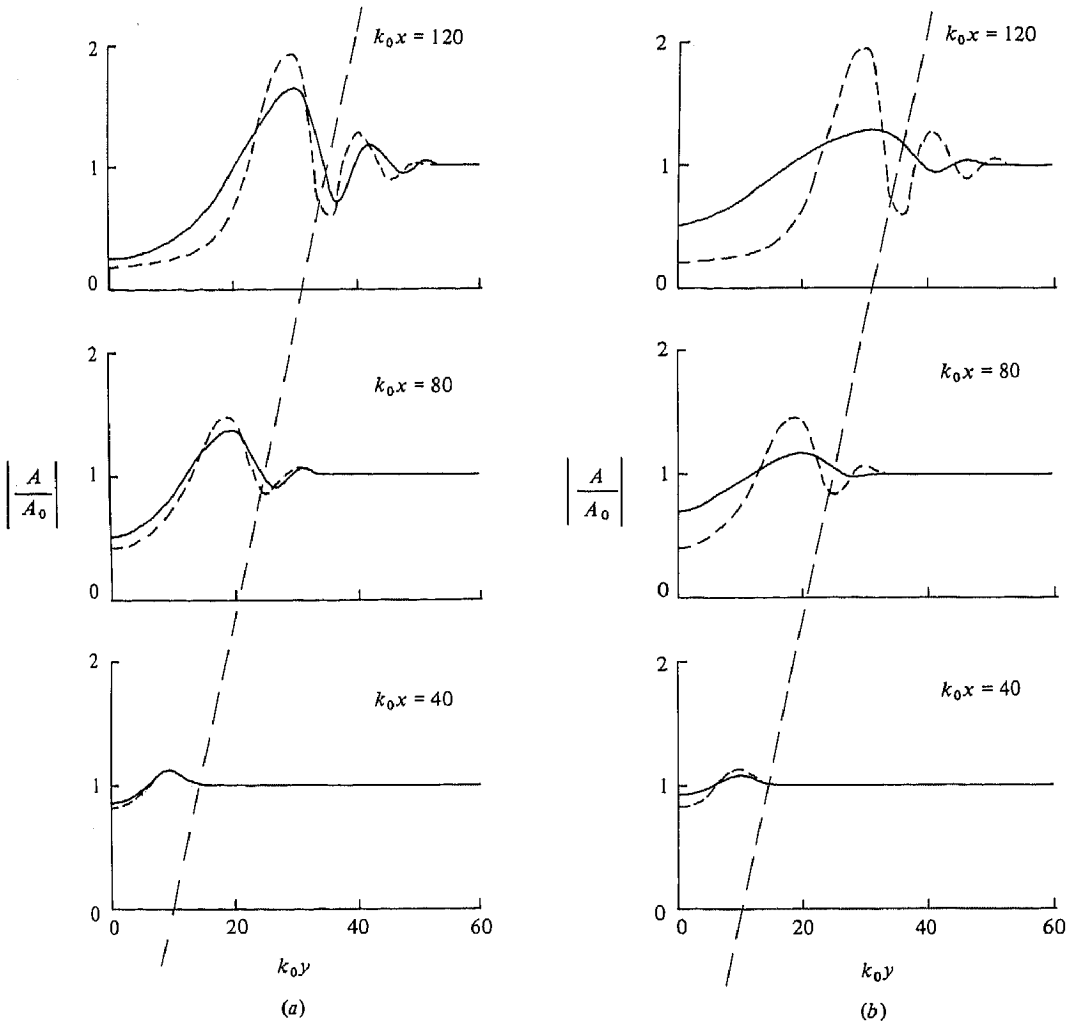

FIGURE 3. Submerged depression, $\alpha = 15°$. Plot of normalized amplitude *vs.* distance from centre of depression: (*a*) $k_0 A_0 = 0.1$; (*b*) $k_0 A_0 = 0.2$; ---, linear theory; ——, solution of (2.22).

with the presence of a reflected wave and a relatively slight reduction of wave amplitude in the neighbourhood of the caustic being apparent. For $\alpha = 15°$ and $k_0 A_0 = 0.2$ (figure 3*b*), however, the reflected wave is not as apparent, and a broad region of waves which are slightly higher than the incident wave develops in the vicinity of the caustic. In addition, wave amplitude decays much more slowly in the linear shadow zone.

The result of nonlinearity is even more accentuated in the results for $\alpha = 25°$, where little reflection of the incident wave is apparent for either incident steepness. In order to accentuate the qualitative differences between the linear and nonlinear results, plots of the instantaneous surface for the linear result and for $k_0 A_0 = 0.2$ are given in figures 5 and 6 respectively, for a wedge angle of $\alpha = 25°$. It is apparent in figure 6 that a broad wave crest travelling parallel to the caustic region has developed. Peregrine (1983) argues that this wave crest must continue to grow in width since

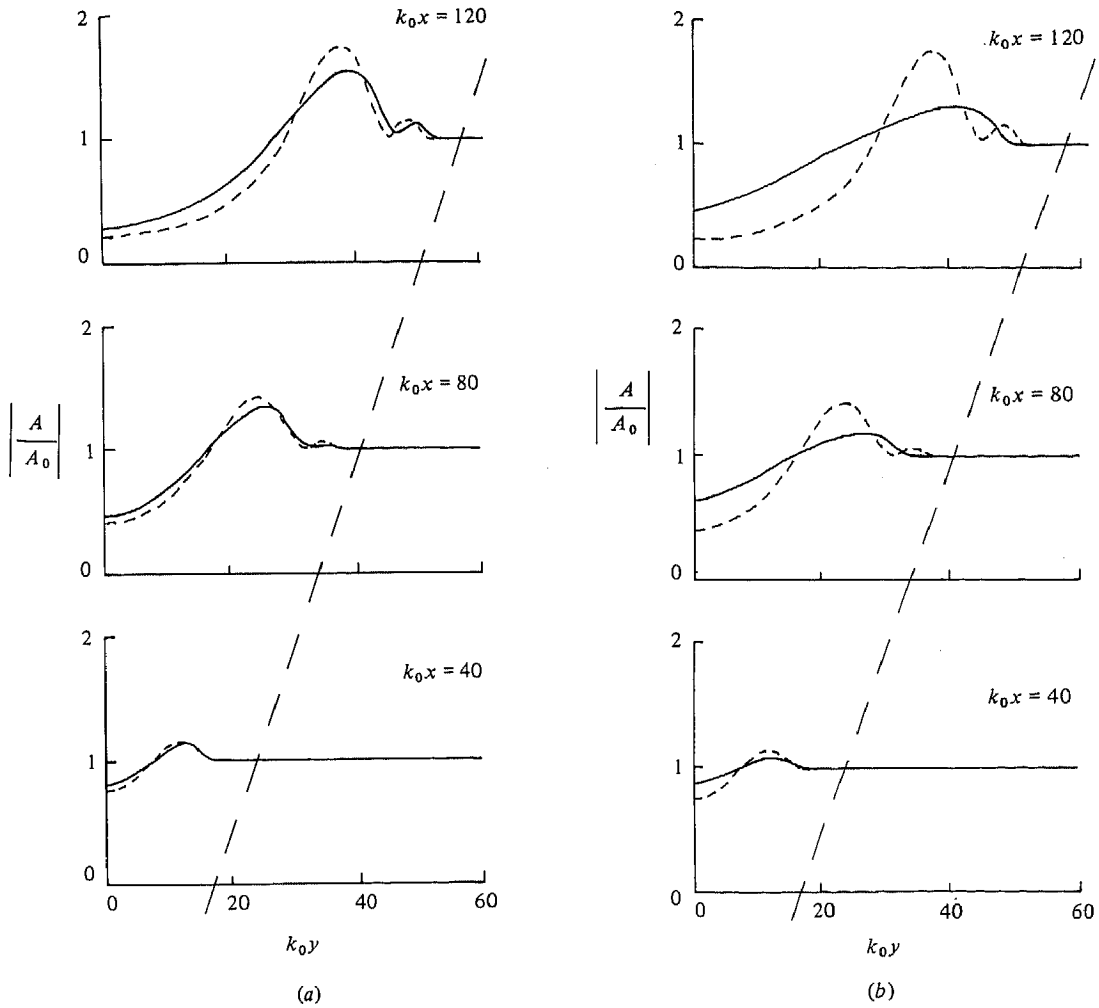

FIGURE 4. Submerged depression, $\alpha = 25°$. Plot of normalized amplitude *vs.* distance from centre of depression: (*a*) $k_0 A_0 = 0.1$; (*b*) $k_0 A_0 = 0.2$; ---, linear theory; ——, solution of (2.22).

the wave energy flux continually incident on the jump boundary cannot be balanced by the flux in a jump of constant width and height unless total reflection of the incident wave occurs. It is therefore unlikely that the wave field will evolve into its asymptotic state.

A possible explanation for the relatively stronger nonlinear effect in the $\alpha = 25°$ cases as compared to the $\alpha = 15°$ cases lies in the increased amount of time (or distance) that the $\alpha = 25°$ wave must spend in the vicinity of the caustic as it is turned and reflected by the refraction process. Results not presented here indicate a similar increase in nonlinear effect when the slope of the bottom is decreased, leading to a spatially slower refraction process and longer residence of waves in the vicinity of the caustic.

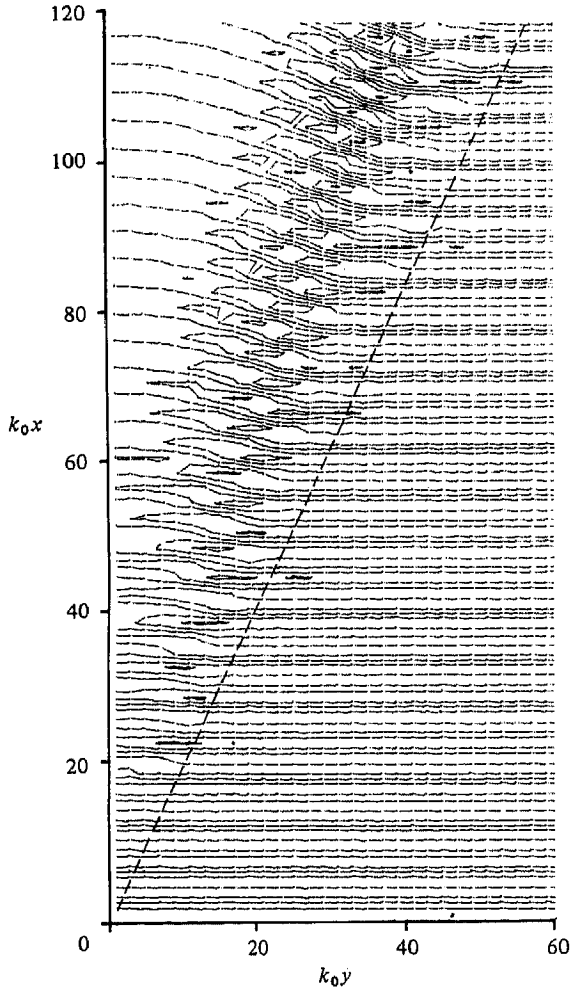

FIGURE 5. Instantaneous surface, linear theory. Contour increments are $0.5A_0$. Inclined line indicates location of top of slope.

5. Discussion

We have shown that the effects of amplitude dispersion and weak wave–wave interaction can significantly alter the structure of a wave field in the vicinity of caustics of the linear theory, where amplification of the incident wave leads to the onset of nonlinear behaviour. In particular, the wave jump between two adjacent wave states, as described by Peregrine (1983) and documented clearly in the Mach-reflection results of Yue & Mei (1980), is seen to occur in several situations where refraction leads to the presence of wavetrains intersecting at small angles. These results have implications for the prediction of wave fields in nature, where irregular bottom topography and current distributions routinely lead to caustics or irregular focusing in the ray approximation. Since principal interest is often focused on the potential effects of storm waves with large steepness, it is possible that the ray theory or even the linear refraction–diffraction correction would result in misleading predictions in some instances.

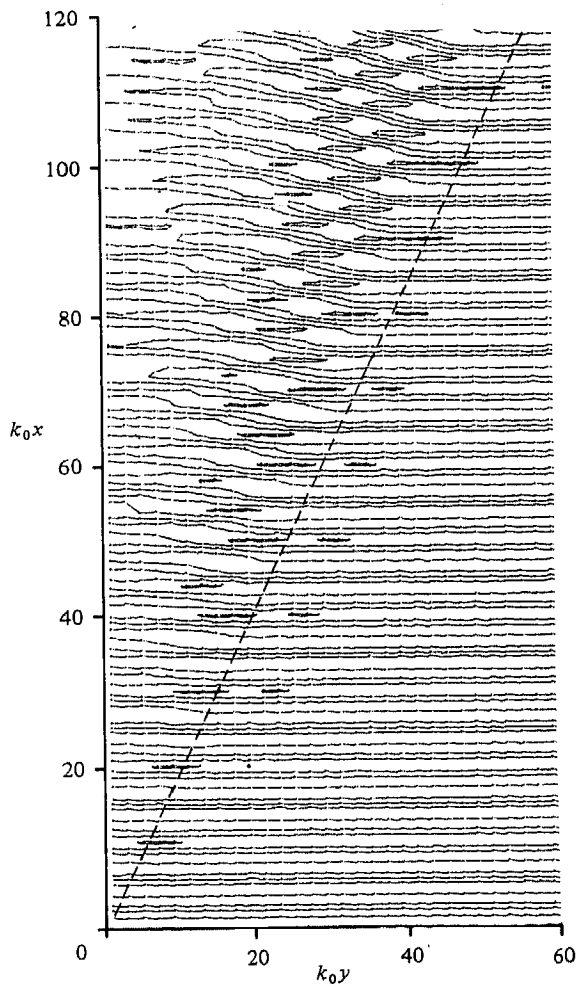

FIGURE 6. Instantaneous surface, $k_0 A_0 = 0.2$, solution of (2.22).

The present theory is, of course, not without its limitations. A principal limitation is that the Schrödinger equation should correctly be used to study modulations occurring over a large number of wavelengths; situations where focusing occurs over the space of only several wavelengths are known to produce free harmonics as the dominant nonlinear effect, and these are not represented in the present theory. Also, the neglect of time dependence of A and the imposition of the slow ($O(\epsilon^2)$) scale for variations in the direction of propagation precludes the study of wave instabilities, such as that of Benjamin & Feir (1967), which may be induced either by the fairly rapid changes in wave conditions at the location of jumps, or by the slow, refraction-induced wave modulations occurring over a slowly varying bottom.

Very little controlled laboratory data exists for the testing of the above predictions. The Mach reflection has been the most heavily investigated phenomenon; see the article by Wiegel (1964) for early results. In the case of waves in the vicinity of caustics, most experimenters have studied small-amplitude waves with the intent of verifying linear wave models; a similar effort may be required in order to provide results applicable to nonlinear models. Several data sets exist which describe waves

focused into a cusped caustic by submerged shoals; these experiments are typically constrained by basin dimensions, and the experimental regions of focused waves typically develop over a small number of wavelengths. Despite this seeming violation of the scaling assumptions involved in the parabolic approximation, preliminary indications are that the parabolic equation is capable of accurately modelling wave amplitudes in regions of relatively rapid focusing. Comparisons with the data of Whalin (1971) (Liu & Tsay 1983*b*) and Berkhoff *et al.* (1982) will be the subject of subsequent investigations.

This work was sponsored by the Office of Naval Research, Coastal Sciences Program. The authors would like to thank Dr D. Howell Peregrine for providing a copy of his manuscript, which provided explanations for several of the effects that were studied here from a purely numerical basis. The authors would also like to acknowledge Prof. Philip L.-F. Liu for his discussions on the subject.

REFERENCES

Benjamin, T. B. & Feir, J. E. 1967 The disintegration of wave trains on deep water. Part 1. Theory. *J. Fluid Mech.* **27**, 417–430.

Berkhoff, J. C. W. 1972 Computation of combined refraction–diffraction. In *Proc. 13th Intl Conf. Coastal Engng, Vancouver.*

Berkhoff, J. C. W., Booij, N. & Radder, A. C. 1982 Verification of numerical wave propagation models for simple harmonic linear water waves. *Coastal Engng* **6**, 255–279.

Chu, V. H. & Mei, C. C. 1970 On slowly-varying Stokes waves. *J. Fluid Mech.* **41**, 873–887.

Corones, J. 1975 Bremmer series that correct parabolic approximations. *J. Math. Anal. Applic.* **50**, 361–372.

Liu, P. L.-F. & Mei, C. C. 1976 Water motion on a beach in the presence of a breakwater. 1. Waves. *J. Geophys. Res.* **81**, 3079–3094.

Liu, P. L.-F. & Tsay, T.-K. 1983*a* On weak reflection of water waves. *J. Fluid Mech.* **131**, 59–71.

Liu, P. L.-F. & Tsay, T.-K. 1983*b* Refraction–diffraction model for weakly nonlinear water waves. Unpublished manuscript.

Lozano, C. & Liu, P. L.-F. 1980 Refraction–diffraction model for linear surface waves. *J. Fluid Mech.* **101**, 705–720.

McDaniel, S. T. 1975 Parabolic approximations for underwater sound propagation. *J. Acoust. Soc. Am.* **58**, 1178–1185.

Mei, C. C. & Tuck, E. O. 1980 Forward scattering by long thin bodies. *SIAM J. Appl. Maths* **39**, 178–191.

Meyer, R. E. 1979 Theory of water-wave refraction. *Adv. Appl. Mech.* **19**, 53–141.

Miles, J. W. 1978 On the second Painlevé transcendent. *Proc. R. Soc. Lond.* A **361**, 277–291.

Peregrine, D. H. 1983 Wave jumps and caustics in the propagation of finite-amplitude water waves. *J. Fluid Mech.* **136**, 435–452.

Radder, A. C. 1979 On the parabolic equation method for water-wave propagation. *J. Fluid Mech.* **95**, 159–176.

Tsay, T.-K. & Liu, P. L.-F. 1982 Numerical solutions of water-wave refraction and diffraction problems in the parabolic approximation. *J. Geophys. Res.* **87**, 7932–7940.

Whalin, R. W. 1971 The limit of applicability of linear wave refraction theory in a convergence zone. R.R.H-71-3, *U.S. Army Corps of Engrs, WES, Vicksburg.*

Wiegel, R. L. 1964 Water wave equivalent of Mach-reflection. In *Proc. 9th Intl Conf. Coastal Engng*, 82–102, *Lisbon.*

Yue, D. K.-P. 1980 Numerical study of Stokes wave diffraction at grazing incidence. Sc.D. dissertation, MIT.

Yue, D. K.-P. & Mei, C. C. 1980 Forward diffraction of Stokes waves by a thin wedge. *J. Fluid Mech.* **99**, 33–52.